American Mineralogist, Volume 64, pages 317–328, 1979

Synthesis and stability relations of Mn–Al piemontite, $Ca_2MnAl_2Si_3O_{12}(OH)$

MARY KESKINEN[1] AND JUHN G. LIOU

Tuttle-Jahns Laboratory for Experimental Petrology
Department of Geology, Stanford University
Stanford, California 94305

Abstract

Stability relations for the Mn–Al piemontite bulk composition $Ca_2MnAl_2Si_3O_{12}(OH)$ were investigated at 1 and 2 kbar and temperatures between 200° and 750°C, using cold-seal pressure apparatus and solid oxygen buffer techniques. Pure piemontite, with average cell dimensions a = 8.86(1), b = 5.69(1), c = 10.19(2)A and β = 115°42′, was readily synthesized from oxide mixtures at 500°–600°C and fO_2 defined by the Cu–Cu_2O and Cu_2O–CuO buffers at 1 and 2 kbar. The high-temperature equivalent assemblage is intermediate grossular-spessartine garnet solid solution [$Ca_2MnAl_2Si_3O_{12}$: a = 11.804(2)A, n_D = 1.7636(2)] + fluid for fO_2 defined by the QFM, HM, CC, and CT buffers. The cell parameters for synthetic piemontites and garnets grown over a range of fO_2 conditions show only small and random variations; this relation suggests that compositional changes of garnet and piemontite for the bulk composition $Pm_{33}Cz_{67}$ with variation of fO_2 are limited. Average measured a for the synthetic garnets is slightly higher than the calculated value for this bulk composition.

In agreement with evidence from natural piemontite-bearing parageneses, reversal runs indicate that crystallization of piemontite requires a high oxygen fugacity. Along the HM buffer, garnet was the only condensed phase stable at all experimental conditions. Equilibrium reversal for the reaction piemontite = garnet + fluid [$Ca_2MnAl_2Si_3O_{12}(OH)$ = $Ca_2MnAl_2Si_3O_{12}$ + 1/2 H_2O + 1/4 O_2] was delineated, for 2 kbar at 617°±10° for the CT buffer, at 404°±10° for the CC buffer, and below 250°C for the HM buffer. At Pfluid = 1 kbar, piemontite is stable up to 591°±10° for the CT buffer and to 402°±10°C for the CC buffer. The effect of fluid pressure on the stability of piemontite is apparently minor compared to that of oxygen fugacity.

The sporadic occurrence of piemontite in a wide variety of geologic environments from blueschist to greenschist and amphibolite facies conditions is mainly controlled by oxygen fugacity in addition to pressure, temperature, and major-element composition of the host rocks. Introduction of Fe into piemontite in natural compositions will evidently result in a more complex breakdown reaction and in an extension of the piemontite stability field to higher temperatures and lower oxygen fugacities.

Introduction

Piemontite, the Mn^{3+} epidote, has been described from a broad spectrum of rock types and geological environments, ranging from blueschist to greenschist and amphibolite facies. A common assertion has been that piemontite is predominantly the product of low-grade metamorphism (Deer *et al.*, 1962; Makanjuola and Howie, 1972). Natural examples support this view: piemontite-bearing metacherts and schists commonly occur in blueschist facies terranes in Japan (Ernst and Seki, 1967, and others), and many greenschist facies piemontites have also been described (Simonson, 1935; Marmo *et al.* 1959; Nayak, 1969; Taylor and Baer, 1973). A more thorough compilation of piemontite localities, however, reveals a significant number of occurrences from rocks metamorphosed under upper greenschist and amphibolite facies conditions (Smith and Albee, 1967; Cooper, 1971; Strensrud, 1973). Similarly, the requirement of a moderately unusual, Mn-rich host rock has also been suggested as an explanation for the restricted development of piemontite, a hypothesis encouraged by the common appearance of piemontite in shear

[1] Present address: Department of Geology, Smith College, Northampton, Massachusetts 01063.

0003-004X/79/0304-0317$02.00

zones affected by "mineralizing" hydrothermal solutions associated with manganese ore deposits (Hutton, 1938; Trask *et al.*, 1942; Taliaferro, 1943; Bilgrami, 1956). However, several studies have indicated that appropriate major-element composition alone, although important, cannot explain piemontite formation (Ernst and Seki, 1967; Smith and Albee, 1967).

This restricted and sporadic occurrence of piemontite suggests that factors other than temperature, pressure, or whole-rock composition control its crystallization. Several lines of evidence from studies of natural parageneses suggest that oxygen fugacity and fluid composition may be critical factors in crystallization of piemontite. Until recently, no experimental work had been done to verify the suggested limitation of piemontite to rocks metamorphosed under highly-oxidizing conditions. The present study is part of an experimental program designed to investigate the stability of piemontite in terms of temperature, pressure, and oxygen fugacity, and to examine the role of manganese on crystal chemistry and stability of the epidote-group minerals in general.

Epidote-group minerals: chemistry and previous studies

Piemontite and associated minerals are characterized by compositional variations within octahedral sites in the basic formula $A_2M_3Si_3O_{12}(OH)$. The seven- or eight-coordinated A site is usually occupied by calcium and perhaps minor Mn^{2+} in the epidotes,

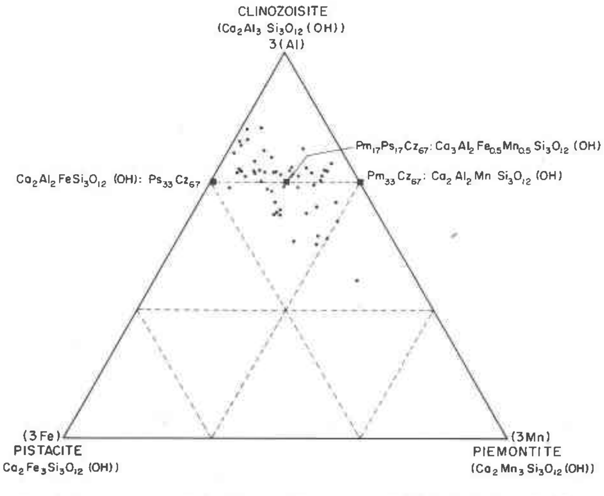

Fig. 1. Extent of solid solution (in terms of Al–Mn–Fe variations within three octahedral sites) for natural piemontites, showing 53 published analyses. Compositions of theoretical end members of epidote minerals and bulk compositions of concern to the present study are also shown.

with Sr, Pb, and lanthanide-series elements occurring in isomorphous allanite. The three nonequivalent octahedral M sites in the epidote structure vary in average bond length and degree of octahedral distortion, a factor important in understanding the crystal chemistry and hence the degree of compositional variation and the stability of piemontite and its coexisting minerals in natural parageneses. These three M sites contain dominantly trivalent with minor divalent ions. Aluminum with very minor iron or manganese (less than 10 percent) characterizes the dimorphous zoisite–clinozoisite mineral pair; aluminum, ferric iron, and minor manganese characterize the epidotes; and high manganese distinguishes the piemontites.

Solid solution between $Ca_2Al_3Si_3O_{12}(OH)$ and $Ca_2(Fe,Mn)_3Si_3O_{12}(OH)$ is not complete; minerals of the epidote group are rarely found with greater than 40 percent replacement of aluminum by ferric iron. The most common extent of solid solution for epidote is usually cited as approximately 33 percent of the pistacite end-member. Compositional variation of natural piemontites is plotted in terms of the ternary Al–Fe–Mn end members in Figure 1. This diagram shows a general compositional restriction of piemontites to greater than 50 percent Al/(Al+Mn+Fe) and to less than 35 percent Mn/(Al+Fe+Mn), a somewhat more extensive compositional variation than is shown by the epidotes (Strens, 1966).

It has been assumed that the behavior of Mn and Fe in the epidote structure is essentially the same, at least in their effects on the relationships between chemical composition and properties such as refractive indices and cell parameters (see discussions by Seki, 1959; Myer, 1966; Strens, 1966). However, the poor correlation of these properties with Fe/(Fe+Al) or (Fe+Mn)/(Al+Mn+Fe) ratios for piemontites and the markedly different pleochroic schemes for piemontites (even those with low Mn contents) from those of epidotes suggest that this assumption is an oversimplification. The reddish-violet–yellow–crimson pleochroism is the distinguishing property of piemontite and is attributed to the presence of trivalent Mn.

Until recently, the only information on the stability of piemontite was that obtained from natural occurrences and by comparison with determined *P*fluid–*T*–fO_2 relations of the other members of the epidote series (Liou, 1973, and others). Piemontite was synthesized by Strens (1964) from oxide mixtures and glasses of unspecified composition seeded with epidote at temperatures of 550° and 650°C and pressures from 2.1 to 4 kbar, but the composition of these piemontites and their stabilities were not determined.

The results of an extensive investigation of synthesis, stability, and physical properties of the Mn^{3+}-bearing silicates, including piemontite, have recently been published (Anastasiou and Langer, 1976, 1977; Langer *et al.*, 1976). Anastasiou and Langer (1977) synthesized piemontites with Al:Mn ratios ranging from 5:1 to 5:7, and described the extent of solid solution of Mn for Al in synthetic piemontites and the variations in physical and optical properties for their synthetic phases. However, their investigations were conducted at very high fO_2 conditions (Mn_2O_3–MnO_2 buffer) and at 7 and 15 kbars fluid pressure.

The present study has attempted to determine the fO_2–T–Pfluid stability relations for a single piemontite composition, $Ca_2MnAl_2Si_3O_{12}(OH)$, which is representative of a "natural" end member of these minerals, $Cz_{67}Pm_{33}$. In order to correlate the experimental conditions as closely as possible with those existing in natural environments for piemontite formation, we have chosen to conduct the experiments at pressures of one and two kbar and in a range of oxygen fugacities reasonably close to those present under natural metamorphic conditions, defined by hematite–magnetite, cuprite–tenorite, and copper–cuprite buffers. An iron-free composition was chosen for initial study in order to determine the effects of manganese on the stability and structure of piemontite without the complicating effects of another transition metal in the system. Choice of this composition also facilitates comparison of these results with the stability relations previously obtained in experimental studies of the epidote composition $Cz_{67}Ps_{33}$ determined by Holdaway (1972) and Liou (1973).

Experimental method

Synthesis and stability relations for piemontite of the composition $Ca_2Al_2MnSi_3O_{12}(OH)$ were investigated hydrothermally, in standard cold-seal pressure vessels with water as the pressure medium. A few reconnaissance runs were conducted using high-pressure cold-seal apparatus and argon as the pressure medium. Pressure was measured with a variety of gauges calibrated against a 30,000 psi Heise gauge, and values cited are believed accurate to within ± 10 bars. Temperatures listed in the run tables (Tables 2 and 5), taking into account accuracies of the chromel–alumel thermocouples, temperature gradients, and the temperature fluctuations imposed by the temperature controllers, are believed accurate to within $\pm 10°C$. The presence of variable-valence elements in piemontite and in the resultant breakdown phases makes it necessary to control oxygen fugacity by the use of solid oxygen buffer techniques. A range of fO_2 conditions within the hematite stability field (HM, CC, CT) was selected for stability studies, as compatible with evidence from natural piemontite occurrences and with the trivalent state of manganese in piemontite. A few reconnaissance runs were performed along the QFM buffer. Abbreviations and compositions of synthetic phases and buffer assemblages used in the text and diagrams are listed in Table 1.

Starting materials for syntheses were prepared by mixing appropriate amounts of oxides and carbonates in the stoichiometric proportions for piemontite. These mixtures were fired at 900°C and one atmosphere for one hour in order to break down the carbonates. For synthesis experiments, these mixtures were sealed with excess H_2O in $Ag_{70}Pd_{30}$ capsules, which in turn were sealed in Ag or Au outer capsules with the buffer mixtures and 30 to 45 microliters of water. For reversal experiments, synthetic piemontite and its high-temperature equivalent assemblage were mixed in subequal proportions as starting materials.

All synthetic phases (except for some metastable assemblages described below) were extremely fine-grained and in many cases poorly crystallized, making optical examination unproductive except for determination of gross homogeneity within the charges. X-ray characterization using slow scans with a Norelco diffractometer (Cu$K\alpha$ radiation, Ni filter) was the sole means available for phase identification; determination of the direction of reaction in reversal runs was made by comparison of peak height ratios from equivalent X-ray scans of starting materials and reversal run products. The unit-cell dimensions of synthetic piemontite and garnet were determined from diffraction scans and Guinier powder patterns and a powdered silicon internal standard and refined

Table 1. Abbreviations and compositions of phases and components used in text and diagrams

Pm = piemontite	end member:	$Ca_2Mn_3Si_3O_{12}(OH)$
	composition studied:	$Ca_2MnAl_2Si_3O_{12}(OH)$
Ps = pistacite	end member:	$Ca_2Fe_3Si_3O_{12}(OH)$
Cz = clinozoisite	end member:	$Ca_2Al_3Si_3O_{12}(OH)$
Gt = garnet	composition studied:	$Ca_2MnAl_2Si_3O_{12}$
Wo = wollastonite		β-$CaSiO_3$
An = anorthite		$CaAl_2Si_2O_8$
F = fluid		
HM = hematite-magnetite buffer		Fe_2O_3-Fe_3O_4
CC = copper-cuprite buffer		Cu-Cu_2O
CT = cuprite-tenorite buffer		Cu_2O-CuO
QFM = quartz-fayalite-magnetite buffer		SiO_2-Fe_2SiO_4-Fe_3O_4

using the least-squares cell-parameter refinement program of Appleman and Evans (1973).

Experiments at such high oxygen fugacities may involve special problems in ensuring that hydrogen is able to diffuse into the inner capsule at a rate adequate to establish equilibrium fO_2 values within the charge. As a check as to whether equilibrium fO_2 conditions were attained, a series of runs was made in which various transition metals or their oxides (*e.g.*, Cu, Cu_2O, CuO, Fe_2O_3) were sealed with H_2O in an AgPd capsule, then enclosed within Au capsules with the various buffer mixtures and water and held at 450°C and 2 kbar for three weeks. For these short run durations and low temperatures, extent of reaction of the inner charge to the metal or oxide appropriate for the predicted fO_2 conditions was always incomplete, suggesting that low reaction and diffusion rates at temperatures less than 450° render results at these conditions suspect. However, for the experiments in this study, run durations of 6 to 10 weeks at low temperatures for reversals are believed to have been of sufficient length so as to minimize if not eliminate this potential problem. Also, all buffer assemblages were X-rayed at the end of the run to ensure both that the buffer was not exhausted and that some conversion of one phase to the other had occurred, thus indicating at least an approach towards equilibrium hydrogen exchange. The consistency of our experimental results even at low temperatures (for example, the conversion of garnet to piemontite at 400°C with the Cu–Cu_2O buffer and of piemontite to garnet at 250°C with the hematite–magnetite buffer) further suggests that run durations were sufficient to lend credibility to all but the lowest-temperature (<300°C) runs, in which the extent of reaction was so slight as to be undetectable.

Table 2. Synthesis run data for piemontite ($Pm_{33}Cz_{67}$) bulk composition+excess H_2O from oxide mixtures

Sample No.	Buffer	Pfluid (Kbar)	Temp. (°C)	Duration (days)	Condensed Run Products
H1-1	CT	1.0	650	5	Pm + An + minor Gt
P1-69	CT	1.0	745	30	Gt + Wo + An + Mn_2O_3
P1-47	CT	1.0	749	7	Pm + Wo + Mn_2O_3
P1-44	CT	1.0	751	7	Wo + An + Mn_2O_3
P1-55	CT	1.0	754	7	Wo + An + Mn_2O_3 + Gt
P1-110	CT	1.5	723	14	Gt + Wo + An + Mn_2O_3
P1-54	CT	2.0	528	7	Pm
P1-16	CT	2.0	550	23	Pm
P1-7	CT	2.0	550	36	Pm
P1-43	CT	2.0	569	7	Pm
P1-34	CT	2.0	569	17	Pm
P1-5	CT	2.0	600	23	Pm
P1-88	CT	2.0	747	11	Coarse gr. Gt + minor Wo
P1-89	CT	2.0	750	11	Coarse grained Gt
P1-28	CT	6.3	570	23	Pm + Gt + minor Mn_2O_3
P1-12	CT	6.3	600	31	Pm + minor Gt
P1-9	CT	6.3	600	25	Pm
P1-3	CT	7.3	600	31	Pm + minor Gt
P1-2	CT	7.9	610	24	Pm + minor Gt
P1-1	CT	8.0	550	25	Pm
P1-10	CC	2.0	550	29	Pm
P1-13	CC	7.9	575	30	Gt
P1-46	None	2.0	571	14	Gt + minor Pm
P1-63	HM	2.0	500	25	Gt
P1-62	HM	2.0	522	12	Gt
P1-26	HM	2.0	569	27	Gt
P1-15	HM	2.0	575	23	Gt
P1-14	HM	2.0	600	23	Gt
P1-11	HM	2.0	600	29	Gt
P1-8	HM	7.7	500	25	Gt
P1-4	HM	7.8	600	28	Gt
P1-6	HM	7.8	600	16	Gt
P1-20	HM	8.2	558	31	Gt

Description of synthetic phases

Piemontite

Piemontite was readily synthesized in the temperature range 400° to 600°C at all pressures with the CC and CT buffers. Synthesis runs at appropriate conditions (Table 2) yielded pure piemontite from oxide mixtures of the bulk composition studied, with no detectable accessory phases. X-ray diffraction patterns identical to that of natural piemontite, complete recrystallization of the charges, the specific bulk composition, and the deep rose-pink color of the powdery charges led to positive identification of the synthetic products as piemontite. A few scarce, slightly larger (20 microns maximum length) piemontite grains which showed the characteristic pinkish-violet to yellow piemontite pleochroism were seen in several charges. These grains were clear with no visible inclusions. The more usual, finer-grained charges appear to be optically homogeneous with an average grain size of less than 2 microns. Cell parameters for the synthetic piemontite and for the other synthetic phases are listed in Tables 3 and 4.

As shown in Table 2, crystallization of piemontite from the oxide mixtures at 1 and 2 kbar was essentially complete when CC and CT buffers were used. At the oxygen fugacity of the hematite–magnetite buffer, garnet was synthesized under all conditions. These results are in some disagreement with the findings of Anastasiou and Langer (1976), who found that piemontite of Al:Mn of 2:1 could not be synthesized at 7 kbar and at oxygen fugacities lower than those of the Mn_3O_4–Mn_2O_3 buffer, which represents more oxidizing conditions than those defined by the CT or CC buffers. Several 6 to 8 kbar syntheses for the present study also yielded a mixture of piemontite plus garnet at temperatures higher than 600°C. Cell parameters for the piemontite of this bulk composition synthesized by Anastasiou and Langer are included in Table 3 for comparison. The average values of a = 8.86(1), b = 5.69(1), c = 10.19(2)A, and β =

Table 3. Cell dimensions of synthetic piemontites [$Ca_2Al_2MnSi_3O_{12}(OH)$] from present and previous studies

Sample No.	Buffer	Temp. (°C)	P_{fluid} (bars)	a_o (Å) (±.01Å)	b_o (Å) (±.01Å)	c_o (Å) (±.02Å)	Volume (Å³) (±0.7Å³)	β (±8')
P1-10	CC	550	2000	8.85	5.68	10.20	462.1	115°35'
P1-63½	CT	524	2000	8.86	5.70	10.19	464.4	115°33'
P1-54	CT	528	2000	8.87	5.71	10.18	464.5	115°40'
P1-1	CT	550	8000	8.85	5.69	10.19	465.7	115°40'
P1-34	CT	569	2000	8.87	5.70	10.21	464.3	115°48'
P1-43	CT	569	2000	8.87	5.70	10.19	464.1	115°48'
P1-27	CT	598	2000	8.85	5.68	10.20	464.4	115°48'
Anastasiou and Langer, 1977.	Mn_2O_3-MnO_2	800	15000	8.839(3)	5.644(2)	10.166(4)	459.0(4)	115°61(3)'

115°42′, obtained for the piemontites in our study, are consistent and are comparable to their synthetic values and to those of natural piemontites.

Garnet

For this bulk composition, the stable breakdown assemblage of piemontite and the product of synthesis experiments at temperatures higher than 608° along the CT buffer and 575°C along the CC buffer at two kbar consists of intermediate spessartine–grossular garnet solid solution+fluid. Along the HM buffer curve, garnet was the only phase obtained at all temperature–pressure conditions. Garnet-bearing charges were usually very fine-grained (less than 2 microns) and whitish pink in color. At high temperatures (750°C) some charges yielded relatively coarse-grained (50–100 microns), euhedral, wine-red garnets with a typical refractive index of 1.7636(2) in Na light. Essentially complete recrystallization of the charges to homogeneous garnet with no detectable accessory phases suggests that the synthetic garnet is probably on composition with the starting mixtures. Mn^{3+}-bearing garnets have been synthesized only at pressures higher than 25 kbar (Strens, 1965; Nishizawa and Koizumi, 1975), and are rarely reported from natural rocks; hence it may be assumed that a charge-balanced garnet of the composition $Ca_2MnAl_2Si_3O_{12}$ would contain predominantly Mn^{2+}.

For garnets synthesized over such a wide range of fO_2 conditions, it might be suspected that the $Mn^{2+}:Mn^{3+}$ ratios would vary. It has been observed, most pertinently by Holdaway in his 1972 study on Fe-bearing epidotes, that gradual compositional changes of reactant and product phases along a breakdown curve may yield a divariant field rather than a univariant line. If this were the case here, the spessartine component of the synthetic garnet would decrease, with a concurrent formation of minor undetectable amounts of one or more compositionally-compensating phases such as Mn_2O_3 or $CaSiO_3$, at high oxygen fugacities. However, in the present system, because of the simple nature of the reaction [basically one phase breaking down to another isochemical (except for oxidation state) single condensed phase] this complication of a stepwise decomposition is apparently avoided. As a check for compositional inhomogeneities, cell dimensions of synthetic garnets crystallized over a range of buffer conditions were determined, and the results are listed in Table 4. A plot of cell edges of garnets against fO_2 of formation is shown in Figure 2B.

It is apparent that the cell edge, which can be closely correlated to composition in garnets, varies only slightly and randomly with fO_2 of crystalliza-

Table 4. Cell edges of synthetic garnets for composition $Ca_2MnAl_2Si_3O_{12}$+fluid

Sample No.	Buffer	Temp. (°C)	P_{fluid} (bars)	Cell edge (a_o) (±.001 Å)	Cell volume (Å³) (±1.0 Å³)
P1-90	CT	751	2000	11.794	1641
P1-88	CT	747	2000	11.803	1644
P1-66	CT	740	2000	11.799	1642
P1-13	CC	575	7900	11.817	1650
P1-6	HM	600	7500	11.804	1644
P1-18	HM	600	2000	11.798	1642
P1-15	HM	575	2000	11.788	1638
P1-26	HM	569	2000	11.794	1640
P1-20	HM	558	8200	11.825	1654
P1-61	HM	556	2000	11.787	1638
P1-63	HM	500	2000	11.795	1641
P1-RI	QFM	500	2000	11.811	1648
Predicted values for this composition (see text):					
Assuming linear variation between end members				11.775 Å	1633
Using regression equation (Novak & Gibbs, 1971)				11.770 Å	1631

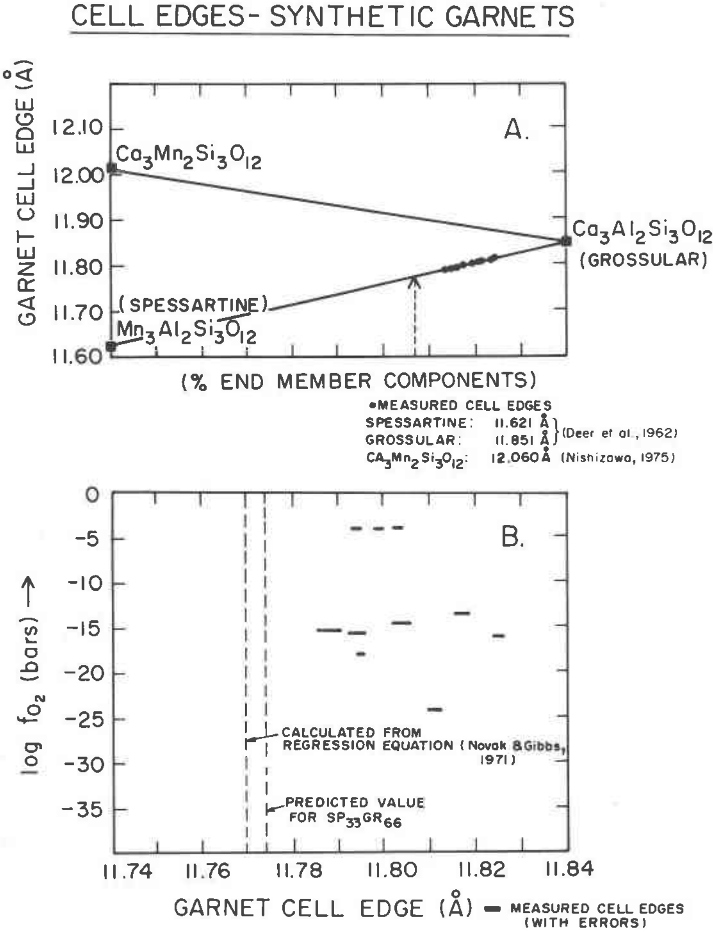

Fig. 2. Plots of cell dimensions of synthetic garnets *vs.* (A) percent theoretical end member components and (B) log fO_2 of formation. Fig. 2A shows predicted cell edge in garnet solid solutions assuming linear variation between spessartine, grossular, and $Ca_3Mn_2Si_3O_{12}$ (Nishizawa and Koizumi, 1975) end members. Measured cell edges of synthetic garnets shown by solid circles. Arrow designates predicted value for garnets of this bulk composition. Fig. 2B shows variation between measured cell edges of garnets from this study versus fO_2 of crystallization. Dotted lines are placed at calculated values for this bulk composition (see text).

tion, with an average value of 11.804(2)A. Comparison of cell parameters of piemontite synthesized at various oxygen fugacities (Table 3) similarly shows no variation, with all values consistent to within ±0.01A. The coarse-grained garnets crystallized at high temperature show slight optical zonation, suggesting that some compositional readjustment may take place during the course of a synthesis run.

It is of interest to compare the measured cell dimensions for these garnets with those predicted either by assuming linear variation of cell edge with grossular–spessartine solid solution using end-member values from Deer *et al.* (1962), or by using the regression equation given by Novak and Gibbs (1971) relating garnet composition to physical properties. The measured values of the synthetic garnets are significantly higher than those predicted for $grossular_{67}$ $spessartine_{33}$, as shown in Table 4 and Figure 2A. This discrepancy may be due to some small degree of variation in $Mn^{2+}:Mn^{3+}$ in comparison to natural garnets, although how both charge balance and bulk composition can be simultaneously maintained remains an unresolved problem. The possibility that some degree of hydration (with a resulting increase in cell edge) might occur in the synthetic garnets, especially those synthesized at low temperatures, cannot be totally discounted. However, the anomalously high and consistent cell edges for garnets grown from 500° to 750°C, temperatures above those at which hydrogarnet components of grossular and spessartine garnets are usually stable (Carlson, 1956; Hsu, 1968), suggest that this phenomenon is most likely not a significant factor. Therefore, synthetic garnets for the reversal experiments described in the later section were prepared at temperatures high enough to preclude significant hydration of the garnets.

Metastable assemblages

Reconnaissance runs at one kbar initially suggested that the phase relations for this bulk composition were somewhat more complex. At 750°C and the fO_2 defined by the CT buffer, a fairly coarse-grained assemblage of β-$CaSiO_3$ (wollastonite)+anorthite+Mn_2O_3 (+ fluid) crystallizes from the oxide mix. At lower fO_2 conditions the high-temperature assemblage at one kbar is again garnet+fluid. Anastasiou and Langer (1977) found that braunite solid solution, together with garnet+fluid, rather than Mn_2O_3, occurred as one of the breakdown products of piemontite. However, X-ray differentiation of these two phases in charges of poor crystallinity cannot be definitive. In subsequent experiments, the three-phase charges were reground and rerun. Under all experimental conditions, garnet or piemontite was found to grow at the expense of this assemblage, indicating that the assemblage wollastonite+anorthite+Mn_2O_3+fluid is metastable. The metastable assemblage probably crystallized as the result of low diffusion rates of hydrogen through the capsule walls at high oxygen fugacities in short-duration runs. The Wo+An+Mn_2O_3 assemblage may form metastably early in the run under anomalously high oxygen-fugacity conditions which would result from the highly oxidized state of the air-fired oxide mixture. The buffer may later be able to impose equilibrium conditions on the charge, and recrystallization to garnet would begin. Such recrystallized garnets might be more coarse-grained as a result of the availability of fewer nucleation sites than were present in the original finely-ground oxide mixtures. Longer runs at one kbar supported this suggested sequence.

Reversal experiments

Reversal experiments were carried out by using finely-ground starting mixtures of subequal amounts of piemontite and the breakdown phase garnet in the presence of excess H_2O. The charges were held at the temperature and pressure of interest for two to four weeks at high temperatures and from four to ten weeks at lower temperatures. For runs at low temperatures and those very close to the equilibrium values, it was sometimes necessary to regrind and rerun a charge at identical P–T–fO_2 conditions before the direction of reaction could be determined with certainty. The experimental results are listed in Table 5 and isobaric fO_2–T relations are shown in Figures 3 and 4 for one and two kbar respectively. The breakdown reaction for this composition is a combination of dehydration and oxidation–reduction as shown below:

$$Ca_2Al_2MnSi_3O_{12}(OH) \rightleftarrows$$
$$Ca_2MnAl_2Si_3O_{12} + 1/2\ H_2O + 1/4\ O_2$$

As mentioned earlier, piemontite of this composition

Table 5. Run data for piemontite stability starting from mineral mixtures. (1) Piemontite+garnet+fluid; (2) Pm+An+Wo+Mn_2O_3+Gt

Run No.	Starting Mix	Temp. (°C)	P_{fluid} (bars)	Buffer	Duration (days)	Results*
P1-R1	(1)	502	2000	QFM	44	Gt
P1-49	(1)	329	1000	HM	28	Gt
P1-41	(1)	405	1000	HM	28	Gt
P1-40	(1)	431	1000	HM	28	Gt
P1-75	(1)	212	2000	HM	57	No react.
P1-58	(1)	258	2000	HM	50	Gt
P1-45	(1)	301	2000	HM	28	Gt
P1-48	(1)	329	2000	HM	28	Gt
P1-39	(1)	357	2000	HM	33	Gt
P1-38	(1)	383	2000	HM	28	Gt
P1-37	(1)	401	2000	HM	28	Gt
P1-36	(1)	429	2000	HM	28	Gt
P1-21	(1)	455	2000	HM	22	Gt
P1-23	(1)	478	2000	HM	22	Gt
P1-24	(1)	502	2000	HM	22	Gt
P1-25	(1)	530	2000	HM	22	Gt
P1-81	(1)	547	2000	HM	2	Gt
P1-91	(1)	750	2000	HM	26	Gt
P1-70	(1)	275	5000	HM	65	No react.
P1-53	(1)	353	5000	HM	35	Gt
P1-94	(1)	371	1000	CC	42	Pm
P1-95	(1)	388	1000	CC	42	No react.
P1-115	(1)	388	1000	CC	56	Pm
P1-124	(1)	392	1000	CC	72	No react.
P1-112	(1)	399	1000	CC	62	Pm
P1-127	(1)	406	1000	CC	33	No react.
P1-153	(1)	410	1000	CC	66	Gt
P1-144	(1)	416	1000	CC	68	Gt
P1-102	(1)	749	1000	CC	22	Gt
P1-98	(1)	757	1000	CC	7	Gt
P1-68	(1)	352	2000	CC	44	Pm
P1-83	(1)	378	2000	CC	29	Pm
P1-84	(1)	396	2000	CC	29	Pm
P1-92	(1)	402	2000	CC	59	Pm
P1-72	(1)	408	2000	CC	48	Gt
P1-60	(1)	411	2000	CC	24	Gt
P1-57	(1)	448	2000	CC	15	Gt
P1-52	(1)	533	2000	CC	15	Gt
P1-50	(1)	544	2000	CC	14	Gt
P1-51	(1)	579	2000	CC	14	Gt
P1-139	(2)	593	1000	CT	15	Pm
P1-136	(2)	602	1000	CT	15	Gt
P1-137	(2)	614	1000	CT	15	Gt
P1-118	(2)	635	1000	CT	15	Gt
P1-135	(2)	704	1000	CT	24	Gt
P1-77	(2)	501	2000	CT	7	Pm + Gt
P1-86	(2)	505	2000	CT	39	Pm
P1-80	(2)	614	2000	CT	7	Pm + Gt
P1-87	(2)	614	2000	CT	36	Pm
P1-116	(1)	626	2000	CT	40	Gt
P1-108	(1)	629	2000	CT	22	Gt
P1-109	(1)	636	2000	CT	22	Gt
P1-82	(2)	652	2000	CT	28	Pm + Gt
P1-114	(1)	659	2000	CT	14	Gt
P1-93	(2)	661	2000	CT	42	Gt
P1-88	(2)	758	2000	CT	36	Gt
P1-85	(1)	764	2000	CT	13	Gt

*Gt (or Pm) growth at the expense of other phases in the starting mixture.

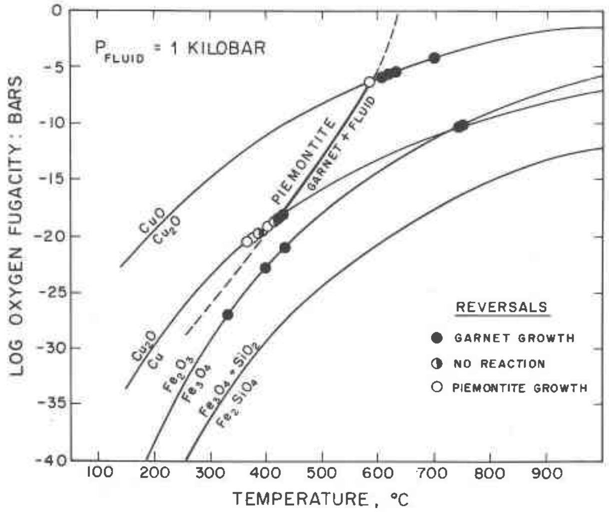

Fig. 3. Log fO_2–T diagram for the piemontite bulk composition, $Ca_2Al_2MnSi_3O_{12}(OH)$ + excess H_2O, at one kbar *P*fluid. Open circles: piemontite growth at the expense of garnet in reversal experiments. Solid circles: garnet growth at the expense of piemontite. Half-filled circles: no apparent reaction. Oxygen buffer curves in this and subsequent figures were calculated according to data by Huebner (1969, 1971) and Kurshakova (1971). Temperatures for reversal experiments are believed accurate to ±10°C.

was synthesized only when buffers more oxidizing than HM were used. Reversal experiments in the range 200°–500°C along the HM buffer were consistent in showing that garnet grew at the expense of piemontite even at temperatures as low as 250°C. The reactions below 250°C are extremely sluggish; therefore, we tentatively conclude that the stability of piemontite may be restricted to below 250° at the fO_2 values defined by the HM buffer and *P*fluid = 2 kbar. With increasing oxygen fugacity, the dehydration temperature increases. The reaction was reversed and bracketed at 617°±10°C for the CT buffer and at 404°±10°C for the CC buffer at two kbar. At one kbar, the reversed breakdown temperatures were 591°±10°C for the CT buffer and 402°±10°C for the CC buffer. The *P*fluid–*T* slope of the reaction is nearly independent of pressure, especially for the CC buffer. This is consistent with a calculated change in volume for this reaction of approximately −4.9±0.3 cm^3/mole (using values for water at 400°C, 1 kbar, from Burnham *et al.*, 1969), which, when combined with the positive change in entropy for a dehydration reaction, suggests a vertical to slightly negative pressure–temperature slope for this piemontite breakdown reaction. The effect of pressure on dehydration temperature for piemontite of this composition is apparently very minor in comparison to the effect of oxygen fugacity.

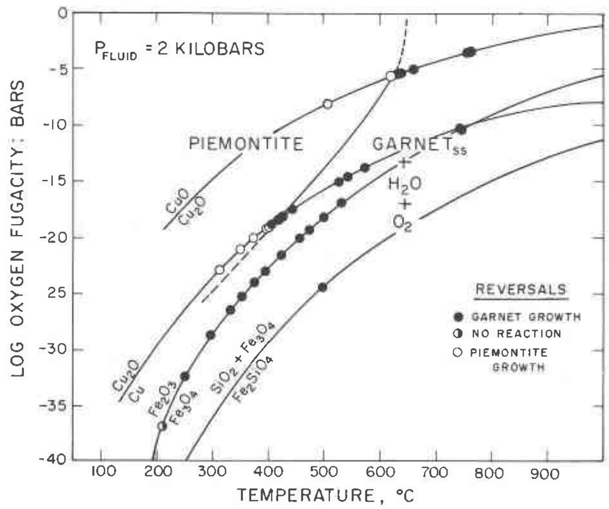

Fig. 4. Log fO_2–T diagram for the piemontite bulk composition, $Ca_2Al_2MnSi_3O_{12}(OH)$+excess H_2O, at two kbars *P*fluid.

Discussion: experimental results

Our experimental results confirm the evidence deduced from natural occurrences that oxidation state during metamorphism represents a major factor in piemontite formation. Comparison of these results with the published stability data on pure Mn–Al piemontites determined by Langer *et al.* (1976) at 7 and 15 kbar indicates that the stability field of piemontite is restricted to significantly lower temperatures for lower oxygen fugacities. The considerably higher pressure at which they performed their study makes comparison of their results to those of the present and of previous epidote-stability studies difficult. Their preliminary work does confirm the decrease of piemontite stability with decreased fO_2. They found that piemontites with compositions along the join piemontite–clinozoisite [$Ca_2Al_{3-p}Mn_pSi_3O_{12}(OH)$] plus excess silica are stable up to melting temperatures in the range of 890° to 940°C at 7 kbar and the fO_2 values defined by the Mn_2O_3–MnO_2 buffer. For piemontite with Mn:Al of 1:2, their work indicated that (1) the breakdown temperature decreases at 7 kbar from 940°C at the fO_2 of the Mn_2O_3–MnO_2 buffer to less than 900° at the fO_2 of the Mn_3O_4–Mn_2O_3 buffer; (2) for fO_2 below that of the CT buffer, piemontite coexists with garnet+anorthite for this bulk composition; and (3) piemontite is unstable with respect to garnet+anorthite at the fO_2 of the Mn_3O_4–MnO buffer (Langer *et al.*, 1976).

They extended their results by comparing their data on piemontite to epidote-stability studies by Holdaway (1972), to make the observation that the Mn^{3+}-bearing phase shows a higher temperature stability. This statement is perhaps justified by their data. However, in the present study, in which experimental conditions were closer to those used in the epidote studies by Liou (1973) and Holdaway (1972), it can definitely be seen that, for geologically realistic physical conditions, pure Mn:Al piemontite is stable only at lower temperatures than are the Al:Fe epidotes (Fig. 5).

The wide temperature range (blueschist through greenschist to amphibolite facies) over which piemontite may occur in nature requires some explanation, in the light of the very low stability temperatures encountered for the piemontite studied here. Addition of pistacite component to the pure Mn–Al piemontite may expand the stability field to lower oxygen fugacities and to higher temperatures. Our results on piemontite stability are compared with those on epidote stability by Liou (1973) in Figure 5. It is apparent that the Mn–Al piemontite is restricted to lower temperatures at oxygen fugacity values (CC, HM buffers) which would already qualify as in the upper fO_2 range for natural conditions of metamorphism. The non-stability of piemontite along the HM buffer curve is in agreement with evidence from natural assemblages, in which piemontite is rarely if ever reported to occur with magnetite. The fact that natural intermediate Fe–Al–Mn piemontites occur over a fairly wide range of metamorphic conditions suggests that increasing substitution of Fe^{3+} will decrease the sensitivity of piemontite to oxygen fugacity, will increase the dehydration temperature, and will shift the stability curve of Fe–Al–Mn piemontite towards that of epidote.

Addition of pistacite component to piemontite would also result in a more complex breakdown reaction similar to that for epidote and once again less dependent on high fO_2. This lessening of fO_2 sensitivity would occur since the studied piemontite $\rightleftarrows$ garnet +fluid reaction is strongly redox in nature, whereas in epidote breakdown ferric iron is present in both the reactant epidote and the products garnet+mag-

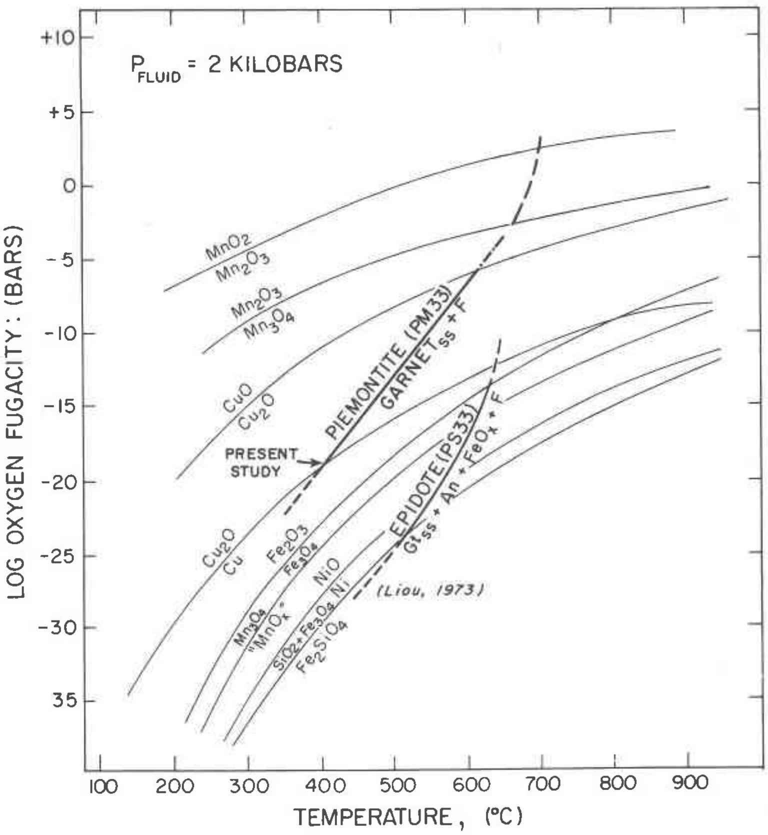

Fig. 5. Log fO_2–T diagram for stability relations of piemontite ($Pm_{33}Cz_{67}$) and of epidote ($Ps_{33}Cz_{67}$), at 2 kbars *P*fluid. Epidote stability by Liou (1973).

netite. Breakdown for an intermediate piemontite may involve gradual compositional changes in coexisting piemontite and garnet along the breakdown curve, with a resultant stepwise reaction such as that suggested for epidotes by Holdaway (1972). We are presently conducting an experimental examination of the stability at one and two kbar of the intermediate piemontite composition $Ca_2Al_2(Mn_{0.5}Fe_{0.5})Si_3O_{12}(OH)$ (see Fig. 1). Preliminary results indicate that both the suggested additional complexities and extended stability field appear to be present for this intermediate piemontite composition.

Discussion: crystal chemistry

Our experimental results are in agreement with petrological evidence concerning the formation of piemontite. They suggest that oxygen fugacity, in addition to temperature, pressure, and major-element composition of the host rocks, is an important factor in controlling the crystallization of piemontite in preference to a manganoan epidote of the yellow-green variety or of another Mn-bearing phase. The relation between high fO_2 and Mn^{3+} in the epidote structure (yielding piemontite) is an obvious one; although many green epidotes in nature may contain higher Mn contents than piemontites from nearby rocks (*e.g.* Smith and Albee, 1967), the substitution of this amount as divalent Mn for Ca is believed to account for the nondevelopment of the characteristic piemontite pleochroic scheme.

The question of how oxidation state affects the site partitioning of transition elements and what minerals form as a result is a complex one for the epidote-group minerals. The effects of Mn on the stability field of epidote must be separated from those of the addition of Fe to piemontite, inasmuch as it might be assumed incorrectly that the effects upon the two solid solutions would eventually converge. However, the Mn in epidote is probably predominantly divalent, the Fe and Mn in piemontite trivalent. Therefore, a piemontite and an epidote may be similar in their cation proportions and yet still be two distinct species.

Crystal-chemical criteria have been used to explain the degree of substitution of Mn and Fe for Al in epidote–piemontite minerals and the apparent extension of the compositional range of these minerals with increasing grade of metamorphism, with an "optimum" substitution of 33 percent (Fe+Mn) in the octahedral sites (Miyashiro and Seki, 1958). The epidote structure contains chains of edge-sharing octahedra parallel to the *b* axis, linked by SiO_4 and Si_2O_7 groups to form five-membered rings. These rings are bound by octahedral cations and by Ca in two approximately trigonal sites with seven- or eight-coordination (Dollase, 1968). The M(3) or between-chain octahedral position is significantly larger and more distorted in its geometry than the two chain octahedral sites, M(1) and M(2). Single-crystal X-ray refinements, as well as Mössbauer and polarized absorption spectral studies (deCoster *et al.*, 1963; Bancroft *et al.*, 1967; Burns and Strens, 1967; Dollase, 1971, 1973), have indicated that in epidote and piemontite Fe and Mn are confined primarily to the M(3) site, a preferred substitution related both to ionic size criteria (Fe and Mn ions have larger ionic radii than Al ions) and to a gain in crystal field stabilization energy due to Mn^{3+} ions in the distorted site. The stability and composition of piemontite or epidote is therefore highly dependent upon the types of ions available, which is in turn controlled by the oxidation state existing at the time of metamorphism. The site environments for these transition metals within other phases, such as garnet, also affect intercrystalline cation partitioning between the phases, whether the relationship between them is one of coexistence or of progressive replacement.

Applications

The breakdown reaction determined in the present study is admittedly greatly oversimplified in terms of natural parageneses. Nevertheless, in natural occurrences, spessartine-rich garnet is commonly associated with piemontite, either as a coexisting phase (Cooper, 1971; Nayak, 1969) or as a breakdown product due to progressively higher temperature and/or increasingly reducing conditions.

Experimental work on transition-metal-bearing geologic systems has repeatedly indicated the importance of oxygen fugacity as a parameter in petrological processes. The occurrence of alternating beds of piemontite- and epidote-bearing rocks of very similar bulk composition has been described numerous times in the geological literature (Mayo, 1933; Gresens and Stensrud, 1977), and this seemingly perplexing variation in paragenesis has been generally attributed to variations in oxidation state during metamorphism. The high oxygen fugacity required for piemontite formation is also compatible as an explanation for unusual cation partitioning involving Fe, Mn, and Mg in rocks like the amphibolite facies interlayered piemontite- and epidote-bearing gneisses described by Smith and Albee (1967). The presence of hematite and of high Fe^{3+} contents in muscovite and phlogopite coexisting with piemontite suggests formation under highly oxidizing conditions. Adjacent epidote-bearing layers contain more common Fe^{2+}-rich assemblages for amphibolite facies gneisses: biotite, ferrous-iron-rich amphibole, hematite, and garnets with significant almandine contents. The elemental compositions of these gneisses, except for valence states, are quite similar despite mineralogical differences; hence the explanation for these two different parageneses requires variation of fO_2 between the layers at the time of metamorphism, an interpretation which this experimental study supports.

Acknowledgments

This research was conducted under funding provided by NSF grant EAR73-06520-A02/Liou. In addition, the first author was supported during part of this research by an NSF Graduate Fellowship. Dr. Philip M. Fenn, Peter Schiffman, and Peter Gordon are warmly thanked for invaluable moral and logistical support, technical assistance, and the proverbial helpful discussions. For above-the-call-of-duty maintenance of the all-important X-ray diffraction equipment as well as valuable consultations concerning collection and reduction of the X-ray data cited in this paper, Dr. Mark Taylor and Keith Keefer are gratefully acknowledged. We also thank Drs. W. G. Ernst, L. C. Hsu, P. M. Fenn, and D. M. Burt for critical readings of the manuscript and for their helpful comments.

References

Anastasiou, P. and K. Langer (1976) Synthese und Stabilität von Piemontit, $Ca_2Al_{3-p}Mn_p(Si_2O_7/SiO_4/O/OH)$. *Fortschr. Mineral., 54*, 3–4.

——— and ——— (1977) Synthesis and physical properties of piemontite, $Ca_2Al_{(3-p)}Mn_p^{3+}(Si_2O_7/SiO_4/O/OH)$. *Contrib. Mineral. Petrol., 60*, 225–245.

Appleman, D. E. and H. Evans (1973) Job 9214: Indexing and least-squares refinement of powder diffraction data. *Natl. Tech. Inf. Serv., U.S. Dep. Commerce, Springfield, Virginia, Document PB-216 188.*

Bancroft, G. M., A. G. Maddock and R. G. Burns (1967) Applications of the Mössbauer effect to silicate mineralogy—I. Iron silicates of known crystal structure. *Geochim. Cosmochim. Acta, 31*, 2219–2246.

Bilgrami, S. A. (1956) Manganese silicate minerals from Chikla, Bhandara District, India. *Mineral. Mag., 31*, 236–244.

Boettcher, A. L. (1970) The system $CaO–Al_2O_3–SiO_2–H_2O$ at high pressures and temperatures. *J. Petrol., 11*, 337–379.

Burnham, C. W., J. R. Holloway and N. F. Davis (1969) The specific volume of water in the range 1000 to 8900 bars, 20° to 900°. *Am. J. Sci., 267A*, 70–95.

Burns, R. G. and R. G. J. Strens (1967) Structural interpretation of polarized absorption spectra of the Al–Fe–Mn–Cr epidotes. *Mineral. Mag., 36*, 204–226.

Carlson, E. T. (1956) Hydrogarnet formation in the system lime–alumina–silica–water. *J. Res. Natl. Bur. Stand., 56*, 327–335.

Cooper, A. F. (1971) Piemontite schists from Haast River, New Zealand. *Mineral. Mag., 38*, 64–71.

deCoster, M., H. Pollak and S. Amelinckx (1963) A study of Mössbauer absorption in iron silicates. *Phys. Status Solidi, 3*, 283–288.

Deer, W. A., R. A. Howie and J. Zussman (1962) *Rock-forming Minerals, Vol. 1.* Wiley, New York.

Dollase, W. A. (1968) Refinement and comparison of the structures of zoisite and clinozoisite. *Am. Mineral., 53*, 1882–1898.

——— (1969) Crystal structure and cation ordering of piemontite *Am. Mineral., 54*, 710–717.

——— (1971) Refinement of the crystal structures of epidote, allanite, and hancockite. *Am. Mineral., 56*, 447–464.

——— (1973) Mössbauer spectra and iron distribution in the epidote group minerals. *Z. Kristallogr., 138*, 41–63.

Ernst, W. G. and Y. Seki (1967) Petrologic comparison of the Franciscan and Sanbagawa metamorphic terranes. *Tectonophysics, 4*, 463–478.

Gresens, R. L. and H. L. Stensrud (1977) More data on red muscovite. *Am. Mineral., 62*, 1245–51.

Holdaway, M. J. (1972) Thermal stability of Al–Fe epidotes as a function of fO_2 and Fe content. *Contrib. Mineral. Petrol., 37*, 307–340.

Hsu, L. C. (1968) Selected phase relationships in the system Al–Mn–Fe–Si–O–H: a model for garnet equilibria. *J. Petrol., 9*, 40–83.

Huebner, J. S. (1969) Stability relations of rhodochrosite in the system manganese–carbon–oxygen. *Am. Mineral., 54*, 457–481.

——— (1971) Buffering techniques for hydrostatic systems at elevated pressures. In G. C. Ulmer, Ed., *Research Techniques for High Pressure and High Temperature*, p. 123–177. Springer-Verlag, New York.

Hutton, C. O. (1938) On the nature of withamite from Glen Coe, Scotland. *Mineral. Mag., 25*, 119–124.

Keskinen, M. (1979) *Experimental Investigation of the Stability Relations, Crystal Chemistry, and Field Occurrences of the Manganese Epidote, Piemontite.* Ph.D. Thesis, Stanford University.

Kurshakova, L. D. (1971) Stability field of hedenbergite on the log P_{O_2}–T diagram. *Geochem. Int., 8*, 340–349.

Langer, K., P. Anastasiou and I. Abs-Wurmbach (1976) Synthesis, stability, and physical properties of Mn^{3+}-bearing silicate minerals. *25th Int. Geol. Congr., Sydney, 1976, Abstr. Vol. 2*, 578–579.

Liou, J. G. (1973) Synthesis and stability relations of epidote, $Ca_2Al_2FeSi_3O_{12}(OH)$. *J. Petrol., 14*, 381–413.

Makanjuola, A. A. and R. A. Howie (1972) The mineralogy of the glaucophane schists and associated rocks from Île de Groix, Brittany, France. *Contrib. Mineral. Petrol., 35*, 83–118.

Marmo, V., K. J. Neuvonen and P. Ojanperä (1959) The piedmontites of Piedmont (Italy), Kajlindongri (India), and Marampa (Sierra Leone). *Bull. Comm. Geol. Finlande, 184*, 11–20.

Mayo, E. B. (1933) Discovery of piedmontite in the Sierra Nevada. *Cal. Div. Mines and Geol. Rep., 29*, 239–243.

Miyashiro, A. and Y. Seki (1958) Enlargement of the composition field of epidote and piemontite with rising temperature. *Am. J. Sci., 256*, 423–430.

Myer, G. H. (1966) New data on zoisite and epidote. *Am. J. Sci., 264*, 364–385.

Nayak, V. K. (1969) Piemontite from the manganese ore deposit of Kajlindongri Mine, Jhabua District, Madhya Pradesh. *Ind. Mineral., 10*, 174–180.

Nishizawa, H. and M. Koizumi (1975) Synthesis and infrared spectra of $Ca_3Mn_2Si_3O_{12}$ and $Cd_3B_2Si_3O_{12}$(B:Al,Ga,Cr,V,Fe,Mn) garnets. *Am. Mineral., 60*, 84–87.

Novak, G. A. and G. V. Gibbs (1971) The crystal chemistry of the silicate garnets. *Am. Mineral., 56*, 791–825.

Seki, Y. (1959) Relation between chemical composition and lattice constants of epidote. *Am. Mineral., 44*, 720–730.

Simonson, R. R. (1935) Piedmontite from Los Angeles County, California. *Am. Mineral., 20,* 737–8.

Smith, D. and A. L. Albee (1967) Petrology of a piemontite-bearing gneiss, San Gorgonio Pass, California. *Contrib. Mineral. Petrol., 16,* 189–203.

Stensrud, H. L. (1973) Does piemontite represent only greenschist facies metamorphism? *Contrib. Mineral. Petrol., 40,* 79–82.

Strens, R. G. J. (1964) Synthesis and properties of piemontite. *Nature, 201,* 175–176.

——— (1965) Instability of the garnet $Ca_3Mn_2Si_3O_{12}$ and the substitution $Mn^{+3} \rightleftarrows Al$. *Mineral. Mag., 35,* 547–550.

——— (1966) Properties of the Al–Fe–Mn epidotes. *Mineral. Mag., 35,* 928–944.

Taliaferro, N. L. (1943) Manganese deposits of the Sierra Nevada, their genesis and metamorphism. *Cal. Div. Mines Bull., 125,* 277–333.

Taylor, F. C. and A. J. Baer (1973) Piemontite-bearing explosion breccia in Archean rocks, Labrador, Newfoundland. *Can. J. Earth Sci., 10,* 1397–1402.

Trask, P. D., I. F. Wilson and F. S. Simons (1942) Manganese deposits of California: a summary report. *Cal. Div. Mines Bull., 125,* 51–215.

Manuscript received, April 7, 1978;
accepted for publication, September 13, 1978.